AD-A216 718

(4)

SECURITY CLASSIFICATION OF THIS PAGE

# REPORT DOCUMENTATION PAGE



| | |
|---|---|
| 1a. REPORT SECURITY CLASSIFICATION: Unclassified | 1b. RESTRICTIVE MARKINGS: None |
| 2a. SECURITY CLASSIFICATION AUTHORITY: | 3. DISTRIBUTION / AVAILABILITY OF REPORT: Unlimited |
| 2b. DECLASSIFICATION / DOWNGRADING SCHEDULE: | |
| 4. PERFORMING ORGANIZATION REPORT NUMBER(S): | 5. MONITORING ORGANIZATION REPORT NUMBER(S): |
| 6a. NAME OF PERFORMING ORGANIZATION: Arizona Board of Regents acting for Arizona State University | 6b. OFFICE SYMBOL (If applicable): 4B293 |
| 6c. ADDRESS (City, State, and ZIP Code): | 7a. NAME OF MONITORING ORGANIZATION: Larry R. Cooper |
| | 7b. ADDRESS (City, State, and ZIP Code): Office of Naval Research, Electronics Division, Code: 1114SS, 800 N. Quincy Street, Arlington, VA 22217-5000 |
| 8a. NAME OF FUNDING / SPONSORING ORGANIZATION: Office of Naval Research (ONR) | 8b. OFFICE SYMBOL (If applicable): |
| | 9. PROCUREMENT INSTRUMENT IDENTIFICATION NUMBER: N00014-87-K-0786 |
| 8c. ADDRESS (City, State, and ZIP Code): Electronics Division, Code: 1114SS, 800 N. Quincy Street, Arlington, VA 22217-5000 | 10. SOURCE OF FUNDING NUMBERS: PROGRAM ELEMENT NO. / PROJECT NO. / TASK NO. / WORK UNIT ACCESSION NO. |

11. TITLE (Include Security Classification)
Transport Effects and Spectroscopy of Defects in Microstructures (Unclassified)

12. PERSONAL AUTHOR(S)
Alfred M. Kriman

| 13a. TYPE OF REPORT | 13b. TIME COVERED | 14. DATE OF REPORT (Year, Month, Day) | 15. PAGE COUNT |
|---|---|---|---|
| Final Technical | FROM 87JUL01 TO 89MAR31 | 89DEC20 | 14+this |

16. SUPPLEMENTARY NOTATION

| 17. COSATI CODES | | | 18. SUBJECT TERMS (Continue on reverse if necessary and identify by block number) |
|---|---|---|---|
| FIELD | GROUP | SUB-GROUP | |
| | | | |
| | | | |

19. ABSTRACT (Continue on reverse if necessary and identify by block number)

Microstructures were studied in the presence of generalized defects, both point repulsive potentials and slit openings in barriers. A number of transport effects were discovered. For isolated defects a resonance was found to occur at the threshold energies of a quantum well. A scaling relation was found for scatterers near single barriers. A rich spectrum of effects was found for single defects near and within double-barrier structures. The electronic analogue of single slit diffraction was shown to exhibit high fringe visibilities.





| 20. DISTRIBUTION / AVAILABILITY OF ABSTRACT | 21. ABSTRACT SECURITY CLASSIFICATION |
|---|---|
| ☒ UNCLASSIFIED/UNLIMITED ☐ SAME AS RPT. ☐ DTIC USERS | |
| 22a. NAME OF RESPONSIBLE INDIVIDUAL: Larry R. Cooper | 22b. TELEPHONE (Include Area Code): (202) 696-4215 / 22c. OFFICE SYMBOL: OCNR 1114SS |

FINAL TECHNICAL REPORT

General Abstract:

Microstructures were studied in the presence of generalized defects, both point repulsive potentials and slit openings in barriers. A number of transport effects were discovered. For isolated defects a resonance was found to occur at the threshold energies of a quantum well. A scaling relation was found for scatterers near single barriers. A rich spectrum of effects was found for single defects near and within double-barrier structures. The electronic analogue of single slit diffraction was shown to exhibit high fringe visibilities.

Written presentations of research results:

"Electronic Transport in Microstructures with Defects," (Master's Thesis of Brent Haukness) - This presents a detailed description of the methods used, with 62 figures (145 pp.). It is available on microfilm from University Microfilms Inc., Ann Arbor, Michigan. Abstract:

The effects of elastic point scatterers on the electronic transport properties of microstructures are examined using a generalized transfer matrix approach. Using a delta-function potential to model a defect, transmission characteristics are calculated for a number of different microstructures. Among these is the double barrier resonant tunneling diode. A number of effects are noticed. These effects depend sensitively on the position of the defect relative to specific features of the potential structure, and a saturation of the effects is noticed with increasing defect strength. Some of the peculiarities of the delta-function defect, are also examined, and a comparison is made to defects modeled with a Gaussian potential.

"Analysis of Electron Diffraction in a Novel Field-Effect Transistor," by A. M. Kriman, G. H. Bernstein, B. S. Haukness and D. K. Ferry. - This original paper was published in Superlattices and Microstructures, Vol. 6, No. 4, pp. 381-386, 1989, and presented as a poster at the 1988 Conference

on Superlattices, Microstructures and Microdevices held in Trieste, Italy. It provides a theoretical analysis of the behavior of the QUADFET device. (The work of G. H. Bernstein and D. K. Ferry, and the work of A. M. Kriman related to this project, were not paid by this contract. The work of Haukness was.) This paper represents calculations related to the main topic of geometric effects in scattering in a number of ways: (i) It provided an "entry level" problem for the student (Haukness) which taught him some of the skills that he was to need in mastering the main project, such as using the CONVEX computer with UNIX operating system and with local plotting facilities. (ii) It involved a microstructure in two dimensions with non-trivial geometry. The situation treated - a long thin barrier with a slit, is in fact a nontrivial microstructure with a defect. The "defect" is a slit which intentionally built into the barrier. (iii) The mathematical approach was closely related to that used to solve the general problem ultimately treated by Haukness. Abstract:

We analyze a field effect transistor whose operation utilizes the quantum diffraction of electrons by a narrow slit in the gate. Calculations are performed using a low-energy conformal mapping technique which does not assume small-angle scattering. It is shown that the device will exhibit far-field quantum diffraction similar in appearance to the Fraunhofer patterns observed in optics. The diffraction pattern can be detected as current collected at a number of narrow Schottky contacts which together comprise a "viewing screen". Fringe visibilities on the order of 0.5 are predicted. A number of applications of the device are discussed.

"Geometric Effects of Scattering in Microstructures," by A. M. Kriman, R. P. Joshi, B. S. Haukness and D. K. Ferry. - This original paper will be published in Solid State Electronics, Vol. 32, No. 12, pp. 1597-1601, 1989, and was presented as a poster at the 1989 Conference on Hot Carriers in Semiconductors held in Scottsdale, Arizona. Abstract:

Transfer Matrix techniques are used to study elastic scattering by point defects embedded in quasi-one-dimensional microstructures. This makes possible an exact analysis of phenomena that arise from breaking

of transverse translation invariance. The dependence of transmission probability on scatterer position is studied for parallel transport in quantum wells and for perpendicular transport across single and double barrier structures. It is found that in laterally confined structures, delta-function and other extremely sharp models of a single defect lead to sharp resonances when such defects are well isolated. Such features are associated with multiple reflections between the lateral confining potential and the defect potential. In single-barrier structures with a single nearby defect, an approximate scaling behavior is found that relates transmission for defects at different distances to that at a fixed distance with different energy scales. In double barrier resonant tunneling diodes (DBRTDs), the position of the transmission peak is affected primarily by defects within the quantum well region. The height of the transmission peak is very sensitive to the positions of defects within that region, acting essentially as a probe of the resonance wave function. Defects in front of a DBRTD also affect the valley current by modifying the longitudinal component of the incident momentum.

Educational accomplishments:

One graduate student, Brent S. Haukness (a U.S. citizen), was hired for the year 1988. As a result primarily of the work that he performed under this contract, he earned a Master's degree in Electrical Engineering. He had offers to attend graduate school toward his Ph.D., but he preferred to enter industry; he accepted an offer from, and has been working since January for Texas Instruments, Inc.

It was not found possible, as envisaged in the original budget, to hire another graduate student with adequate qualifications to perform work required under the contract. Instead, Ravindra P. Joshi, who had recently received his Ph.D. in Electrical Engineering from Arizona State University, was hired on a part-time basis. (He worked full-time over all, as he also worked part-time for R. O. Grondin.) This work constituted post-doctoral training allowed under his visa, and it did significantly increase the breadth of his experience beyond what he had learned as a graduate student.

# EFFECTIVE POTENTIAL FOR MOMENT-METHOD SIMULATION OF QUANTUM DEVICES

A. M. Kriman, J.-R. Zhou, N. C. Kluksdahl, H. H. Choi, and D. K. Ferry

Center for Solid State Electronics Research
Arizona State University, Tempe, Arizona 85287-6206

## ABSTRACT

In the simulation of submicron devices, complete quantum descriptions can be extremely computationally intensive, and reduced descriptions are desirable. One such description utilizes a few low-order moments of the momentum distribution that are defined by the Wigner function. Two major difficulties occur in applying this moment method: (i) An independent calculation is required to find quantum mechanically accurate initial conditions. (ii) For a system in a mixed state, the hierarchy of time evolution equations for the moments does not close. We describe an approach to solve these problems. The initial distribution is determined in equilibrium by means of a new effective potential, chosen for its ability to treat the sharp potential features which occur in heterostructures. It accurately describes barrier penetration and repulsion, as well as quantum broadening of the momentum distribution. The moment equation hierarchy is closed at the level of the second-moment time evolution equation, using a closure that is exact for a shifted Fermi distribution. Band-bending is included by simultaneous self-consistent determination of all the moments.

## KEYWORDS

Submicron device simulation; quantum barrier repulsion and penetration; moment method.

## INTRODUCTION

The development of nanometer-scale electronic devices has required the modeling of quantum mechanical effects in device simulations. A number of such simulations have been developed for the resonant tunneling diode (RTD), whose operation depends essentially on the purely quantum mechanical effect of barrier tunneling. Because the RTD is a quasi-one-dimensional device, its analysis is numerically tractable, even when "self-consistency" (electrostatic fields due to mobile charge redistribution) is included (Kluksdahl *et al.*, 1989). More general devices, whose active regions cannot be treated in a one-dimensional approximation, present a computational challenge.

These computational problems already occur in the simulation of classical (non-quantum mechanical) devices. Classical devices are adequately described by the single-particle distribution function which gives the density in the six-dimensional phase space of momentum and space coordinates. Near equilibrium, the momentum distribution at each point is well approximated by a shifted equilibrium distribution. This observation leads to the successful and widely used "moment method" (Blötekjær, 1966 and 1970). In this approach, instead of determining the full distribution function as a function of six arguments, one uses a reduced description based on a few momentum integrals – moments of the distribution function – as functions of spatial position. The moments obey time evolution equations ("moment equations") that are integrals of the Boltzmann equation.

The quantum mechanical generalization of the classical distribution function is the Wigner distribution function, a partial Fourier transform of the density matrix. Iafrate, Grubin and Ferry (1981) developed a quantum generalization of the moment method, based on integrals of the Wigner function. Interestingly, the first three quantum moment equations are formally identical to the classical ones. Thus, if quantum effects are to be included in the simulation, then they must already be present in the initial conditions. This fact is also known from simulations based directly on the Wigner function (Carruthers and Zachariason, 1983): For motion in a parabolic potential, the full classical and quantum distribution functions obey identical equations of motion, so the difference between classical and quantum behaviors must be "contained" in the initial distribution. While this demonstrates that some aspects of the quantum/classical distinction must be contained in the initial conditions, it is nevertheless the case that for motion in general potentials, the classical and quantum evolution equations *also* differ.

The moment equations form a hierarchy, with the time derivative of each moment determined in part by the gradient of the next moment in the hierarchy. In a practical calculation, one computes only a few low-order moments, closing the hierarchy by making some approximation for the highest moment used. Such an approach is justified by the fact that at equilibrium, the exact distribution is completely determined by the density and temperature (the zeroth and second moments). Away from equilibrium, the closure approximation corresponds to an assumption regarding the form of a quasi-equilibrium distribution. In our simulations, we use the first three moments (number, momentum, and energy densities). Our closure is initially derived by assuming that third moments are small, but it is exactly true for a large class of distribution functions, including the shifted Fermi-Dirac distribution.

In one-dimensional RTD models, it is possible to compute a completely self-consistent Wigner distribution function in equilibrium by performing a thermally weighted sum over all states. This has provided an initial distribution which is accurately stationary under numerical integration of the Wigner function time evolution equation. In contrast, a three-dimensional device has many more states, and if its Schrödinger equation is not separable, it is difficult even to find individual states, let alone perform a complete sum. Another method, based on path integrals, does provide a systematic approach, but it too is computationally intensive, and has to date been applied primarily to one-dimensional problems. [See Mason and Hess, (1989), Register *et al.* (1988), and references therein.] What is therefore required is a computationally efficient way of determining an equilibrium (initial) distribution, or set of moments, that would complement the

computationally efficient moment method. As noted, the moments so determined must manifest quantum mechanical effects: quantum mechanical corrections cannot arise independently from the time evolution equations.

Some of the authors (Kriman, Zhou and Ferry, 1989) have recently proposed a statistical ("effective potential") method. This provides a quantum mechanically accurate equilibrium distribution which we will use to satisfy the requirement for accurate initial conditions. The effective potential describes barrier penetration and repulsion, along with equilibrium broadening of the momentum distribution which does not occur classically. Other effective potentials, derived rigorously as semiclassical approximations of the partition function, cannot be applied in the presence to typical device models. Indeed, these previous effective potentials diverge everywhere if the potential is infinite in any finite region. The new effective potential is a well-behaved functional of the real potential, and has the proper asymptotic behavior near an infinite potential barrier, giving errors in density at the few per cent level. Like previous effective potentials, it also approaches the correct high-temperature limits. In the following, we will recapitulate the method and outline its derivation.

## EFFECTIVE POTENTIAL

We find an initial condition in equilibrium by using a recently developed effective potential method (Kriman, Zhou and Ferry, 1989). This method is similar in form to earlier statistical approximations developed by Giachetti and Tognetti (1985; 1986) and by Kleinert (1986) with Feynman (1986). In common with these, the new method computes the density classically from an effective potential which incorporates a local average of the actual potential. The local average represents the quantum position uncertainty of a particle whose energy – and thus momentum – is not completely uncertain. The information about the energy distribution arises from the finite temperature, and thus the range over which the position must be averaged is of the order of the thermal wavelength $\lambda_{TH} \equiv \hbar \sqrt{\beta/2m}$ .

The main respects in which earlier effective potential methods differ from the one we use here have to do with the effect of infinite potentials. The Giachetti-Tognetti and Feynman-Kleinert effective potential approaches assume that the underlying potential is smooth, and proceed from there to derive analytically approximations which are exact in the high-temperature limit. This is supported by the fact that in the high temperature limit, the lowest-order quantum correction to the density is of relative order $\beta(\lambda_{TH})^2 V''$, where $V''$ is the second derivative of the potential (Husimi, 1940). Many of the potentials commonly used in modeling solid state – and particularly heterostructure – devices, contain potentials that are not smooth. The extreme case of this is the infinite wall potential, used where appropriate to set the density to zero.

The previous effective potentials all diverge for this potential, as they do for any potential whose integral in any finite region is infinite. This is because the effective potentials are linear averages of the real potential, and the weighting in space falls smoothly to zero. The new potential method that we have introduced uses nonlinear averages, and remains well-defined in the presence of infinite barriers.

The nonlinear effective potential is derived in the spirit of density functional theory (DFT) (Jones and Gunnarsson, 1989). The DFT is based on the fact (Hohenberg and Kohn, 1964; Levy, 1979; Mermin, 1965) that the electron energy is a unique functional of the electron density. Although the exact functional is unknown and presumably quite complex (Lieb, 1982), it is possible to develop approximate functionals that are adjusted to be quite accurate for a set of simplified cases (Kohn and Sham, 1965). Analogously, the nonlinear effective potential is based on the observation that the density is (by construction) a unique functional of the potential. While the exact formal expression of this functional can be difficult to evaluate, it is again possible to develop approximate functionals by adjusting parameters in a suitable Ansatz. We have also used certain simple, exact properties of the density to constrain the form of the effective potential. These constraints were that (a) the effective potential approach the real one at high temperature, and that the effective potential preserve (b) homogeneity and (c) separability properties of the real potential.

The high-temperature constraint stems from one motivation of effective potentials in general: that in the classical regime the density is given simply by an exponential of the real potential, and that this regime is approached at high temperatures. One simple consequence of this constraint is that various weighting functions must be normalized. Another is that the local averaging must occur over length scales that decrease with increasing temperature. By dimensional analysis, for a sharp potential feature this length scale must be essentially the thermal wavelength.

The homogeneity constraint we impose is that a constant change in the real potential lead to an equal change in the effective potential. This is a surprisingly stringent constraint. For example, consider the potential has the general functional form

$$V_{\alpha}(x) \equiv h_{\alpha}^{-1}\left( \langle h_{\alpha}(V) \rangle(x) \right) , \tag{1}$$

where $h_{\alpha}$ is a function with inverse $h_{\alpha}^{-1}$ under composition:

$$f(x) \equiv h_{\alpha}^{-1}\left( h_{\alpha}(f)(x) \right) . \tag{2}$$

Here h is a real function of a real argument, and nonlocality is introduced by the average $\langle \cdot \rangle(x)$. It can be proven that only two forms of h are allowable in (1) under the constraint of homogeneity. These are $h_L(v) \equiv v$, which leads to the ordinary arithmetic (linear) average, and $h_\gamma(v) \equiv \exp(-\gamma v)$, which leads to the exponential averages that we must ultimately use if infinite potentials are to be admissable. (Slightly more general h's are allowable, but lead to the same averages.)

The separability constraint we use is that if a potential is separable in Cartesian coordinates, then its effective potential will be likewise separable. This property follows from the factorizability of the density when the potential is separable. The weak condition imposed is not sufficient to imply that separability will be conserved for the other coordinate systems in which the Schrödinger equation is separable. However, by means of a standard argument from the kinetic theory of gases, it does follow that averages such as the one appearing in (1) must be defined by a weighting function that is Gaussian. (See, for example, (Castellan, 1971)).

Numerical parameters in the effective potential were set by optimizing the fit to the density in semi-infinite wall potential, whose density is known exactly (Kriman, Kluksdahl, Ferry, 1987). The temperature and mass can be scaled out of this potential, so the results have a very general validity. After requiring that the leading asymptotic behavior of the density near the wall be given exactly (which in itself rules out many functional forms for the effective potential), the maximum fractional error was minimized. Choosing the form

$$\bar{\nabla}(x) \equiv \int_0^\infty \frac{d\gamma}{\beta}\, w(\gamma/\beta)\, \nabla_\gamma(x)\,, \tag{3}$$

with

$$w(s) = w_0 \exp(-\alpha s^2 + \delta s)\,, \tag{4}$$

we found that $w_0$=1.4427, $\alpha$=14.9442, and $\delta$=5.8265. The weight in the average defining $\nabla_\gamma$ is a Gaussian of rms width $2\sigma = 3.3220\lambda_{TH}(\gamma/\beta)^{1/2}$. It should be understood that these four parameters are the result of a two-parameter optimization: (i) The small-$x$ asymptotic behavior of the density ($\rho \sim x^2$) requires $w(0) = (\ln 2)^{-1}$. (ii) The high-temperature/classical-limit constraint requires w to be normalized, so $\delta$ depends on $\alpha$ in a way that has nothing to do with the model potential chosen for optimization. The peak in the distribution w occurs when $\sigma = 0.733\lambda_{TH}$. Thus, the effective potential represents an average of the real potential over a range comparable to the thermal wavelength. (This was expected, but it was not imposed as an independent condition.)

We used this effective potential to compute the density in equilibrium of a resonant tunneling diode. The diode consists of 0.3eV barriers, 5nm long, separated by a quantum well region 5nm long. The electron is assumed to have the a mass 0.067 times the free electron mass, appropriate for GaAs. In Fig. 1 the result of the effective potential calculation is compared with the exact numerical result (Kluksdahl, *et al.*, 1989), computed by summing over scattering eigenstates.

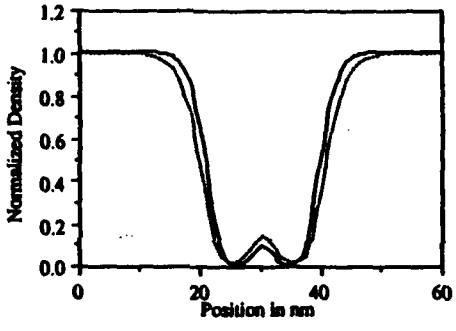


Fig. 1. Electron density from exact approach (sum over scattering states, full line) and effective potential (broken line).

## MOMENT METHOD

A reduced description of semiconductor systems that has been successful for classical problems is the moment method (Blötekjær, 1966 and 1970). In quantum problems, the analogue of the distribution function, which provides a "complete" single-particle description is the Wigner distribution function (Brittin and Chappell, (1962); Carruthers and Zachariason, (1983); Balazs and Jennings, (1984); Hillery, *et al.* (1984)). It is a Fourier transform of the density matrix $\rho(x,x') \equiv \langle \psi^\dagger(x)\psi(x') \rangle$ [$\psi^\dagger$ and $\psi$ are field operators], taken with respect to the difference coordinate:

$$f_W(x,p,t) = \int_{-\infty}^{\infty} dy\, e^{ipy/\hbar}\, \rho\left(x+\tfrac{y}{2}, x-\tfrac{y}{2}\right)\,. \tag{5}$$

The Wigner distribution function $f_W$ is the Weyl transform of the classical single particle phase space density. That is, it is a particular quantum generalization of the phase space density. It is a real function, and one can immediately define local moments of the momentum distribution by

$$\mu_n(x) \equiv \int_{-\infty}^{\infty} dp\, f_W(x,p,t)\, p^n \tag{6}$$

related to local averages of the momentum and its powers by

$$\langle p^n \rangle = \mu_n/\rho\,, \tag{7}$$

where $\rho \equiv \mu_0$. It is possible to derive, from the exact quantum mechanical equation of motion of the Wigner function, a set of *moment* equations analogous to the moment equations of classical semiconductor problems (Iafrate, Grubin and Ferry, 1981). The first three moments evolve in time according to

$$\begin{aligned} &\frac{\partial \rho}{\partial t} + \frac{1}{m}\frac{\partial}{\partial x}\mu_1 = 0\,, \\ &\frac{\partial \mu_1}{\partial t} + \frac{1}{m}\frac{\partial}{\partial x}\mu_2 + \rho\frac{\partial V}{\partial x} = \langle F \rangle\,, \\ &\frac{\partial \mu_2}{\partial t} + \frac{1}{m}\frac{\partial}{\partial x}\mu_3 + 2\mu_1\frac{\partial V}{\partial x} = \langle \dot{E}_K \rangle, \end{aligned} \tag{8}$$

where the inhomogeneous terms on the right contain the effects of collisions. One may reasonably expect that for a good approximation of a statistical system's behavior, it would suffice to evolve just the first three elements, corresponding to density, momentum, and energy. However, as noted earlier, closing the hierarchy at any finite order requires some extra information, typically in the form of an expression, using lower-order moments, of the highest-order moment appearing in the equations. In particular, the last of our moment equations involves the gradient of $\mu_3$, for which no time evolution equation is given. One way of "closing" the moment equations is to make some approximation within the derivation of the moment equations. In this implicit approach, a separate closure expression may not occur, and the approximation is built into the time evolution equations, which are also usually referred to as ("the") moment equations. To remove any ambiguity, let us state that where we refer, in this paper, to the formal equivalence between the first three classical and quantum moment equations, we are referring specifically to (8), the moment equations derived without any hierarchy-closing Ansatz.

In the special case of a pure state, the "statistical" system is described completely by two real quantities: $\psi = \mathrm{Re}(\psi) + i\,\mathrm{Im}(\psi)$. Thus one expects that it should be possible to close the moment equations at the level of the two moments. In fact, Iafrate and coworkers (1981) have shown that for a pure state,

$$\mu_2 = \frac{\mu_1^2}{\rho} - \frac{\hbar^2}{4}\rho\frac{\partial^2}{\partial x^2}\ln\rho\,.$$

The second term is (up to a multiplicative factor) the "quantum potential" of Bohm, and using this closure in the first two equations of the hierarchy (8) yields the same moments as a direct solution of the Schrödinger equation.
For the general (mixed state) case, we first derive our closure expression by regarding the skewness of the momentum distribution as small. We write

$$p = \langle p \rangle + \delta\,,$$

and find that $\langle \delta^2 \rangle = \langle p^2 \rangle - \langle p \rangle^2$, and of course $\langle \delta \rangle = 0$. If we make the assumption of approximately Gaussian distributions, or some other weaker assumption which causes the skewness $\langle \delta^3 \rangle$ to vanish, then we can conclude that

$$\langle p^3 \rangle = 3\langle p^2 \rangle \langle p \rangle - 2\langle p \rangle^3\,. \tag{9}$$

This closure rule has a very useful property: It is easily demonstrated that a large class of distributions, including the common drifted Maxwellian and drifted Fermi distributions, satisfy this relation. In general, it holds for any distribution of the form $f(x,p,t) = F(x,(p-\langle p(x,t)\rangle)^2,t)$.

It is important to note that while the form of our closure is $\langle (p-\langle p \rangle)^3 \rangle = 0$ in the classical case, different closures arise when similar-appearing approximations are made in different contexts. In particular, Ploszajczak and Rhoades-Brown (1985) and Stroscio (1986) use an implicit closure that is essentially equivalent to setting $\langle (p-\langle p \rangle)^3 \rangle = \langle (p-\langle p \rangle)^4 \rangle = 0$ and solving the moment equation for $\mu_3$ [the lowest-order equation *not* shown in (8)]. The closure obtained in this way does contain a quantum correction. However, there as in most perturbative aproaches, increasing orders of $\hbar$ are associated with increasing orders of derivatives of the potential, making it inappropriate for the problems we wish to treat.

## SUMMARY

We have proposed an approach to the moment method for quantum devices, using an effective potential-based density which is designed to mimic important features of the true density, such as tunneling, barrier penetration, and the complementary barrier repulsion. The choice of potential functional is guided by the requirement to satisfy a number of fundamental constraints. We describe an explicit closure for the moment equations at the level of the kinetic energy time evolution equation which is satisfied exactly by all "drifted" distributions.


## ACKNOWLEDGMENT

This work was supported in part by the Army Research Office.

## REFERENCES


Balazs, N. L., and B. K. Jennings, (1984). *Phys. Repts.*, 104, 347-391.
Blötekjær, K., (1966). *Ericsson Tech.*, 2, 127-183.
Blötekjær, K., (1970). *IEEE Trans. Electron Dev.*, 17, 38-47.
Brittin, W. E., and W. H. Chappell, (1962). *Revs. Mod. Phys.*, 34, 620-627.
Carlsson, A. E., and N. W. Ashcroft (1982). *Phys. Rev., B* 25, 3474-3481.
Carruthers, P., and F. Zachariason, (1983). *Rev. Mod. Phys.*, 55, 245-285.
Castellan, G. W., (1971). Physical Chemistry, 2nd. edn., (Addison-Wesley, Reading).
Feynman, R. P., and H. Kleinert, (1986). *Phys. Rev. A*, 34, 5080-5084.
Giachetti, R., and V. Tognetti, (1985). *Phys. Rev. Lett.*, 55, 912-915.
Giachetti, R., and V. Tognetti, (1986). *Phys. Rev. B*, 33, 7647-7658.
Hillery, M., R. F. O'Connell, M. O. Scully and E. P. Wigner, (1984). *Phys. Repts.*, 106, 121-167.
Hohenberg, P., and W. Kohn, (1964). *Phys. Rev.*, 136, B864-871.
Husimi, K., (1940). *Procs. Phys. Math. Soc. Jpn.*, 22, 264.
Iafrate, G. J., H. L. Grubin, and D. K. Ferry, (1981). *J. Physique*, 42 Coll. C7, 307-312.
Kleinert, H., (1986). *Phys. Lett. A*, 118, 267-270.
Kluksdahl, N. C., A. M. Kriman, D. K. Ferry and C. Ringhofer, (1989). *Phys. Rev. B*, 39, 7720-7735.
Kohn, W. and L. J. Sham, (1965). *Phys. Rev.*, 140, A1133–1138.
Kriman, A. M., N. C. Kluksdahl, and D. K. Ferry, (1987). *Phys. Rev. B*, 36, 5953-5959.
Kriman, A. M., J. Zhou, and D. K. Ferry, (1989). *Phys. Lett. A*, 138, 8-12.
Levy, M., (1979). *Procs. Nat. Acad. Sci. (USA)*, 76, 6062-6065.
Mason, B. A., and K. Hess, (1989). *Phys. Rev. B*, 39, 5051-5069.
Mermin, D., (1965). *Phys. Rev.*, 137, A1441-1443.
Register, L. F., M. A. Stroscio, and M. A. Littlejohn, (1988). *Superlatt. Microstr.*, 4, 61-68.
Ploszajczak, M., and M. J. Rhoades-Brown, (1985). *Phys. Rev. Lett.*, 55, 147-149.
Stroscio, M. A., (1986). *Superlatt. Microstr.*, 2, 83-87.

# ANALYSIS OF ELECTRON DIFFRACTION IN A NOVEL FIELD-EFFECT TRANSISTOR

A. M. Kriman*, G. H. Bernstein†, B. S. Haukness* and D.K. Ferry*

*Center for Solid State Electronics Research
Arizona State University
Tempe, AZ 85287-6206

†Department of Electrical and Computer Engineering
University of Notre Dame
Notre Dame, IN 46556

(Received August 18, 1988)
(Revision received June 12, 1989)

We analyze a field effect transistor whose operation utilizes the quantum diffraction of electrons by a narrow slit in the gate. Calculations are performed using a low-energy conformal mapping technique which does not assume small-angle scattering. It is shown that the device will exhibit far-field quantum diffraction similar in appearance to the Fraunhofer patterns observed in optics. The diffraction pattern can be detected as current collected at a number of narrow Schottky contacts which together comprise a "viewing screen". Fringe visibilities on the order of 0.5 are predicted. A number of applications of the device are discussed.

## 1. Introduction

Refinements in nanolithography and epitaxial growth techniques have made possible devices with progressively smaller features, allowing the observation of real-space wave properties of electrons in the solid state. Paradigmatic examples of these are resonant tunneling diodes [1] and small ring structures [2] exhibiting Aharonov-Bohm effects [3]. The signature of the wave mechanical effects is typically some non-monotonic feature in a plot of current versus electric or magnetic field. Such features arise as the interference between different electron paths alternates between predominantly constructive and predominantly destructive.

In at least two respects, the devices that have been made or suggested thus far generally test only special cases of interference phenomena. First, with only one exception that we are aware of (Furuya [4]), there have been no *diffraction* devices, such as gratings or slits, in which "bright" and "dark" regions may be observed *simultaneously*. While electron diffraction has been demonstrated and utilized [5] for measurement, the diffraction pattern is generally detected a macroscopic distance from the diffracting structure, rather than within the microscopic region that produces it.

Second, the interference is usually between quantum paths which differ in some discrete way, as in an Aharonov-Bohm ring, rather than among a continuous range of paths, as in single-slit diffraction. In a path integral view, for instance, the resonant tunneling diode operates by the interference between paths differing in the number of times they traverse the quantum well. In the Aharonov-Bohm rings, the interfering paths differ discretely in their winding number around the flux enclosed by the ring. In the device proposed by Furuya, diffraction is effected by a transverse potential grating in the base, and the paths are distinguished by the opening of the base through which they cross.

We describe a device which differs from existing devices in both of the above-described respects. This "QUADFET" (Quantum Diffraction FET) [6] is essentially a single-slit diffraction experiment realized within the two-dimensional electron gas of an inverted HEMT layer. The analog of the viewing screen is a set of forward-biased Schottky contacts, or "collectors", which serve as the drain (see Fig. 1). The slit width can be varied by adjusting the gate potential, and lobes of the diffraction pattern are detected as variations in the current reaching different collectors.

It is important to consider the survival of the diffraction pattern in the presence of collisions. Beenakker *et al.* [7] performed elegant experiments which show that elastic collisions can be ignored over path lengths of at least 3 μm. Their results demonstrated not only that the phase memory of the electrons was conserved, but also that the elastic collisions did not cause the paths to deviate significantly. If elastic collisions did cause significant deviation of the path, then the Fraunhofer diffraction pattern in the QUADFET would be washed out by the collisions within an elastic mean free path length.

This paper is concerned primarily with how the QUADFET would work in the absence of scattering. A more central problem is whether the device can be made to work given the fundamental differences between the usual optical diffraction experiment and the electronic device we have proposed.

0749-6036/89/080381 + 06 $02.00/0

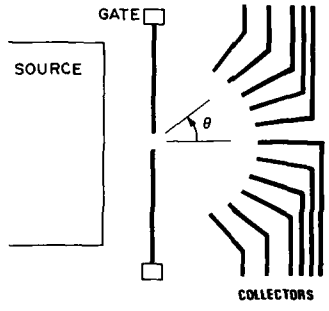


Fig. 1. Top view of the QUADFET.

The first difference is in the source: it is difficult to monochromate and focus electrons in a semiconductor device, whereas optical devices benefit from readily available laser sources shining through transparent, nondispersive media. While some monochromation is possible by the interposition of a gate, in the manner of the THETA device [8], this brings into play the constraint of statistics. Because electrons are fermions, their density in phase space is bounded (by $2/h^3$ on a coarse grain). Thus, focussing and monochromation diminish the current, so it is useful to design a device which functions well with an unfiltered source distribution.

It is clear, therefore, that we must deal with a spatially extended source having a distribution of energies. These give rise to space- and time-domain "coherence" effects which have been studied in ordinary light optics [9,10]. In the specific examples that are usually considered, however, some kind of small-angle approximation is usually made. Without some such approximation, the usual Huygens-Fresnel-Kirchoff approach becomes complicated. Therefore, in analyzing the QUADFET we have developed a new approach related to those used in waveguide analysis.

## 2. Device Model and Diffraction Amplitudes

Our central problem is to give an adequate treatment of the quantum states in the vicinity of the slit. Initially, therefore, we solve the Schrödinger equation for a potential that consists of a single slit gate lying along the $y$ axis:

$$V(x,y) = V_0(y)\,\delta(x), \tag{1}$$

($x$ is the coordinate perpendicular to the gate, within the two-dimensional electron gas), where we consider the special case

$$V_0(y) = \begin{cases} 0 & \text{for } |y| < a/2 \\ \infty & \text{for } |y| \geq a/2 \end{cases} . \tag{2}$$

The gate is assumed, like the corresponding optical barrier, to be infinitesimally thin (i.e., $\propto \delta(x)$). This is justified if the Fermi wavelength is long compared to the actual gate length. The barrier "strength" $V_0(y)$ is nonnegative, so there are no bound states. Thus, a basis of eigenstates for this potential consists of scattering states incident from the right and left. Completely general momentum-normalized [11] left-incident states can be written (using continuity of the wavefunction at $x = 0$) in the form [12]

$$\Psi_{\mathbf{k}}(x,y) = \frac{i}{\pi}\sin(k_x x)\exp(ik_y y)\,\Theta(-x) + \Sigma_{\mathbf{k}} , \tag{3}$$

where $\Theta(u) = \{\ 1 \text{ if } u > 0,\ 0 \text{ if } u \leq 0\ \}$ is the unit step function, and

$$\Sigma_{\mathbf{k}}(x,y) = \frac{k_x}{2\pi}\int dq_y\, F(q_y,k_y;E)\exp(iq_x|x|+iq_y y) . \tag{4}$$

(The integration, here and wherever explicit bounds are not given, is over the whole real line.) This eigenstate describes an electron incident with wave vector $\mathbf{k} = (k_x, k_y)$ (where $k_x > 0$). The sine term in (3) is the standing wave that arises if there is perfect specular reflection at $x = 0$. The difference between this and the exact wavefunction is $\Sigma_{\mathbf{k}}$, which contains components scattered into final wave vectors $\mathbf{q} = (q_x, q_y)$. Because our chosen potential (2) reflects specularly almost everywhere, the correction $\Sigma_{\mathbf{k}}$ goes to zero quickly with increasing distance from the slit, and $F$ is a smooth function of $q_y$. For a permeable ($V_0(y) < \infty$) or rough gate potential, $F$ would have a component proportional to $\delta(q_y - k_y)$, implying finite probabilities for transmission and nonspecular reflection.

The electron generally is scattered with transverse wave vectors taking the full range of values $-\infty < q_y < \infty$. The total energy $E = \hbar^2 k^2/2m$ is conserved ($k \equiv |\mathbf{k}|$), so $\mathbf{q}^2 = k^2$, which makes $q_x$ an implicit double-valued function of $q_y$ for a given energy. The sign of $q_x$ must be chosen to satisfy the scattering boundary conditions: $\Sigma_{\mathbf{k}}$ should have waves propagating away from the gate ($q_x > 0$ when $|q_y| < k$), or exponentially damped away from the slit ($-iq_x > 0$ when $|q_y| > k$). Note that although they do not contribute to the current, these exponentially damped waves are an essential part of the state, and contribute to the density near the gate. (By reflection symmetry, the right-incident states have an expression similar to Eq. (3).)

The scattering state (3) is completely specified by $F$. An earlier study [12] concerned with idealized contacts treated a geometrically similar problem. Generalizing the method developed there (see in particular the case treated in the Appendix), one can write down an implicit solution for a potential of the general form (1): $F$ is that function which satisfies

$$\int dq_y\, F(q_y,k_y;E)\left(q_x + \frac{i}{2}V_0(y)\right)\exp[i(q_y-k_y)y] = 1 \tag{5}$$

for all $y$.

In the earlier study, it was found that the dominant behavior of transmission amplitudes (to $q_y$ from $k_y$) arose from the $k_x$ factor in (4), while the energy-dependence of $F$ was a higher-order effect. In order to keep the problem tractable, therefore, we have assumed

$$F(q_y,k_y;E) \equiv F(q_y,k_y;0) \equiv F(q_y,k_y) . \tag{6}$$

This approximation is completely analogous to one made in calculations of microwave waveguide characteristics [13] and of fluid flow around obstacles and through constrictions [14]. The computational advantage of this approach is the possibility of applying conformal mapping techniques, as we shall do. We apply a mapping into elliptic coordinates

$$\mu + i\xi \equiv w = \cosh^{-1}(2iz/a)\,, \tag{7}$$

with $z = x + iy$.

The infinite barriers of the gate now coincide with $\xi$=0 ($x = 0$, $y < -a/2$) and $\xi = \pi$ ($x = 0$, $y > a/2$). We can now implement the potential simply as a Neumann ($\Psi = 0$) boundary condition, and we can expand $\Sigma_{\mathbf{k}}$ in the complete, *discrete* basis of separated states that results:

$$\Sigma_{\mathbf{k}} = \sum_{n=1}^{\infty} c_n^{(\pm)} \sin(n\xi)\, e^{-n\mu}, \tag{8}$$

where the superscript labels the half-plane of $x$: $c_n^{(\pm)} = c_n^{(+)}$ for $0 < \xi < \pi$ ($x > 0$), and $c_n^{(-)}$ for $\pi < \xi < 2\pi$ ($x < 0$). These expansion coefficients are implicitly functions of $\mathbf{k} = (ik_y, k_y)$; and can be determined by continuity conditions at the slit (the locus $x = 0$, $|y| < a/2$ is just $\mu = 0$). Continuity of the wavefunction immediately implies $c_n^{(+)} = c_n^{(-)} \equiv c_n$. Derivative continuity takes the form

$$-\frac{\partial}{\partial\mu}\Psi(\mu{=}0+,\xi) = +\frac{\partial}{\partial\mu}\Psi(\mu{=}0+,2\pi-\xi)\,.$$

Inserting (3), we find

$$c_n = \frac{n}{\pi} i^{n-1} J_n(k_y a/2)\,, \tag{9}$$

where $J_n$ is the $n^{\text{th}}$-order Bessel function of the first kind [15]. By identifying (4) and (8), and taking Fourier components, we find that

$$F(q_y,k_y) = \frac{i}{(q_y k_y)} \sum_{n=1}^{\infty} n(-1)^n J_n(k_y a/2)\, J_n(q_y a/2)\,. \tag{10}$$

We will be concerned with diffraction patterns in the Fraunhofer regime: current will be collected many wavelengths away from the slit. As noted earlier, $F$ is a smooth function of $q_y$, so we can use a stationary phase analysis of (4) in this regime to find that the wavefunction is asymptotically

$$\Psi_{\mathbf{k}}(x{=}r\cos\theta, y{=}r\sin\theta) \sim k_x \left(\frac{k}{2\pi r}\right)^{1/2} F(k\sin\theta,k_y)\cos\theta \exp[i(kr-\tfrac{\pi}{4})]\,. \tag{11}$$

in polar coordinates; the expression is valid at large distances. More precisely, it is valid whenever $\sqrt{k/r}\cos\theta$ is much smaller than the $q_y$-scale for variations in $F(q_y, k_y)$ about $q_y = k\sin\theta$. Therefore, we make no small-angle approximation, either in our far-field analysis, based on (11), or in our solution of the Schrödinger equation for the scattering states (3).

## 3. Device Characteristics

As discussed in section 1, ballistic paths on the order of 3 microns have been obtained in GaAs/AlGaAs HEMTs at low temperatures. This is considerably longer than the wavelength of a 1 meV electron, and also longer than the minimum feature sizes achievable by electron beam lithography [16]. Because of this, it is possible to choose the dimensions of the drain region in Fig. 1 so as to fulfill two complementary conditions: on the one hand, the collectors are close enough that a large fraction of the electrons travel ballistically from slit gate to drain. On the other hand, they are far enough away that a Fraunhofer diffraction pattern is detected. This can be achieved by placing the tips of the collectors one micron from the slit. With a 100 nm pitch, collectors at this distance would yield an angular resolution of about 6 degrees.

In order to observe diffraction effects, the slit width must be comparable to the electron de Broglie wavelength. This in turn requires a treatment of the states that is based directly on the Schrödinger equation (Section 2). Having placed the collectors in the Fraunhofer regime of distances from the slit, however, we assure that the potential, which depends on the source-drain bias $V_{DS}$, varies with a characteristic length scale much longer than the wavelength. This allows us to retain one simplifying assumption of the usual semiclassical approach to electronic transport: it is possible to neglect the field in the computation of the eigenstates. That is, we can use the states of the previous section. In this regime, the dependence of the current on $V_{DS}$ arises from variation of the state occupation probabilities.

We can assign an occupation probability to the scattering states (3) by observing that their incident current density is the same as that of normalized momentum eigenstates far from the slit [11]. Furthermore, we observe that in equilibrium (zero bias) there is no net current, since the current transmitted through the slit from scattering states incident from the source at any energy is exactly compensated by a deficit of reflected current associated with degenerate scattering states incident from the drain. The net current density in the drain region therefore depends only on the excess occupation probability in the drain:

$$j(\theta) = \int dk_y \int_0^{\infty} dk_x\ \delta n(\mathbf{k})\, j(\theta;\mathbf{k})\,. \tag{12}$$

Here $j(\theta)d\theta$ is that part of the total transmitted current which is ejected into the range of angles ($\theta$, $\theta$+d$\theta$). The current density associated with incident wave vector $\mathbf{k}$,

$$j(\theta;\mathbf{k}) = \frac{e\hbar}{\pi m}\cos^2\theta\, k_x^2\, \mathbf{k}^2\, |F(k\sin\theta,k_y)|^2\,, \tag{13}$$

is computed from (11). With a forward bias of $V_{DS}$, the differential occupation probability is

$$\delta n(\mathbf{k}) = n(E(\mathbf{k}){-}eV_{DS}) - n(E(\mathbf{k}))\,, \tag{14}$$

with

$$n(E) = \frac{2}{1+\exp(E-E_F)}\,.$$

We have evaluated (12) numerically. Figure 2 shows the result for a slit width of 250 nm, an electron density $n = 3 \times 10^{11}$ cm$^{-2}$, and $V_{DS}$ = 0.1 mV. Lobes, characteristic of diffraction, can be seen clearly.

The distribution (14) has a width of roughly $eV_{DS}$ + kT in energy. For a density of $3 \times 10^{11}$ cm$^{-2}$ in n-GaAs, $E_F$ = 11 meV, compared to kT = 0.36 meV (at 4.2K). The electron distribution can therefore be made approximately monochromatic if the bias is kept in the few-millivolt range,

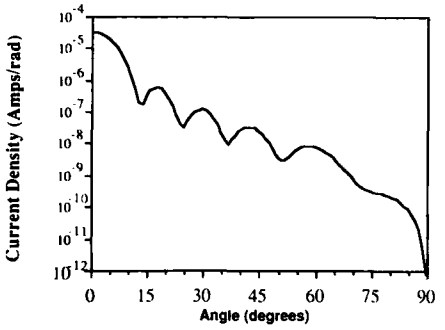


Fig. 2. Angular current density $j(\theta)$ for a slit width of 250 nm, an electron density $n = 3 \times 10^{11}$ cm$^{-2}$, and $V_{DS} = 0.1$ mV.

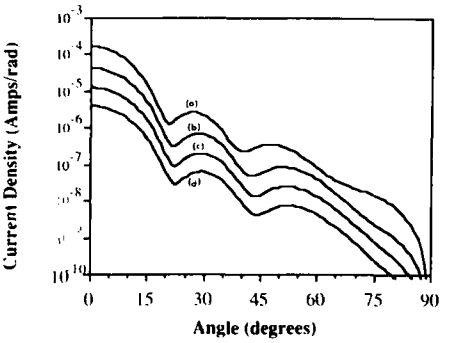


Fig. 3. Current density $j(\theta)$ for a slit width of 150 nm and electron density $n = 3 \times 10^{11}$ cm$^{-2}$, for biases $V_{DS}$ of (a) 3.16 mV, (b) 1.0 mV, (c) 0.316 mV and (d) 0.1 mV.

and for $V_{DS}$ in this range, the temperature dependence due to the width of (14) is negligible (our calculations are performed at T = 0K). Thus, obtaining high temporal coherence is not difficult. Curves in Fig. 3, plotted for different values of the bias, show that for $V_{DS}$ less than about 1 mV, the current density is essentially proportional to bias. At the highest bias, the diffraction lobes are shifted toward smaller angles. This is due to the shorter wavelength of electrons injected at high bias. (Calculations in subsequent figures were performed using $V_{DS} = 0.1$ mV.)

The above suggests that there is only a weak dependence on temperature below about 40K. In the real device, scattering will broaden any sharp features that (12) may exhibit. Nevertheless, studies using hot electron injectors with variable injection energy [8] display a pattern that simplifies our analysis: over short distances, the scattered (non-ballistic) component of the electron distribution quickly assumes a broad distribution of energies, initially very flat over the whole range of energies from zero up to the energy of the ballistic electrons. This kind of scattered component gives rise to a smooth, featureless background, above which the diffraction pattern due to ballistic electrons should be observable.

Another source of incoherence is the spatial extent of the source. A common measure of coherence (appropriate for quasi-monochromatic sources) is Michelson's fringe visibility $V$ [10]. This is defined in terms of the intensities of an adjacent pair of extrema in the diffraction pattern as

$$V \equiv \frac{j_{max} - j_{min}}{j_{max} + j_{min}}. \qquad (15)$$

The most commonly studied example of spatial coherence effects considers a double slit experiment, where the canonical result is that $V$ depends on a quantity $\phi a/\lambda$, where $\phi$ is the angle subtended by the source as viewed from the diffracting slit, and equals $\pi$ for the device shown in Fig. 1. Diffraction fringes are clearly discernible only when $\phi a/\lambda$ is small: $V = |\mathrm{sinc}(\pi\phi a/\lambda)|$ ($\mathrm{sinc}(x) \equiv \sin(x)/x$). Applying this classical result to our situation, for $n = 3\times10^{11}$ cm$^{-2}$ ($\lambda_F = 46$ nm) and $a = 250$ nm, we find $V < 0.02$. In fact, this criterion is rather conservative, because it is derived in the paraxial approximation of small $\phi$ and relatively large $a/\lambda$. This allows one to ignore the disclination factor in Kirchoff's rigorous formulation of the Huygens-Fresnel theory, and to neglect the reduced apparent size of the slit as viewed from an oblique source. The effect of these neglected factors is to reduce the contribution of electron waves incident at wide angles, and effectively focus the incident waves into a source distribution with smaller effective extent $\phi$.

For the present small $a/\lambda$ situation, $j_{max}$ varies rapidly from one peak to the next, so $V$ is ambiguously defined. For a conservative estimate, we compare the current density of each minimum with that at the *subsequent* maximum (i.e., the lower of the two adjacent peaks). In Fig. 4 we plot the resulting fringe visibilities for the lobes of Fig. 2, and find a fairly high value of $V \sim 0.5$. It is unclear at present to what extent these higher values of $V$ are due to our basic approximation (6). However, it seems likely that the classical value 0.02 may be regarded as a lower bound.

## 4. Device Applications

The QUADFET has interesting device applications. Two of these are based on the way the diffraction pattern varies with gate bias. As gate bias is increased, and slit width decreases, the diffraction pattern (Fig. 5) and its lobes (Fig. 6) shift outward to larger angles. Viewed at a particular collector, this leads to oscillations in the current, as different lobes cross the collector's angular position. This

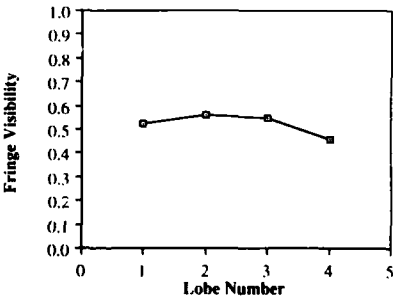


Fig. 4. Fringe visibilities $V$ for the 250 nm slit.

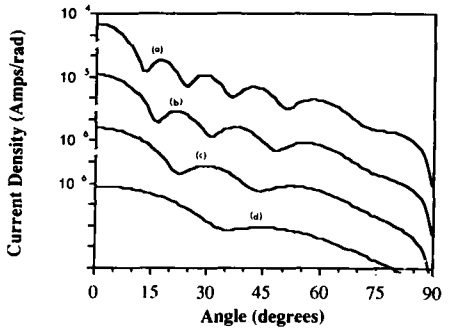


Fig. 5. Current densities for slit widths of (a) 250 nm, (b) 200 nm, (c) 150 nm and (d) 100 nm, for the density and bias conditions of Fig. 1.

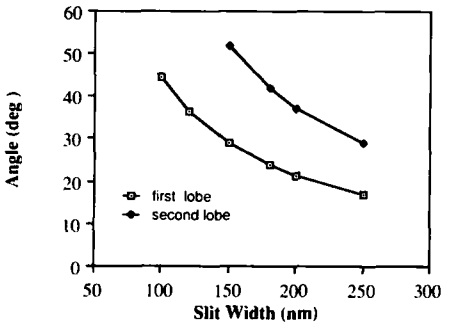


Fig. 6. Positions of the first and second subsidiary current maxima, as functions of the slit width.

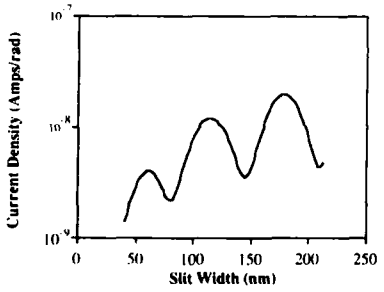


Fig. 7. Current density at 45° viewed as a function of slit width.

phenomenon, shown in Fig. 7, is essentially an oscillatory transconductance. The oscillatory characteristic makes possible a versatile frequency multiplier: for a large angle or voltage amplitude, one cycle of gate voltage can correspond to many cycles of output current. The output has a dominant component at an adjustable frequency, unlike ordinary frequency multipliers, in which the output power is typically shared by a range of harmonics and the output signal must be selected by filtering. Since the device is ballistic and can operate at high frequencies, multiplied frequencies can range into the terahertz under proper conditions of bias, density and angle.

In addition, collectors can be chosen which are turned on or off in complementary response to the input voltage, allowing the formation of a low-power gate. Complementary logic may thus be implemented with QUADFETs in place of the MOSFETs used in CMOS. Possible advantages are a reduced number of fabrication steps and the inherent high speed of ballistic transport.

Furthermore, QUADFETs may be used as magnetic field sensors. A magnetic field applied perpendicular to the plane of the device curves the electron trajectories, shifting and deforming the current pattern detected at the drain collectors.

## 5. Summary

We have described the analysis of a novel field effect transistor, whose operating principle is the quantum diffraction of electrons. Appreciable fringe visibilities can be obtained even in the presence of low source coherence. The useful property of oscillatory transconductance was demonstrated theoretically. This property leads to a number of useful device applications.

**Acknowledgment** - The authors would like to thank S. Bandyopadhyay, E. W. Greeneich and N. C. Kluksdahl for useful discussions. This work was supported in part by the Office of Naval Research.

## References

[1] R. Tsu and L. Esaki, *Applied Physics Letters* **22**, 562 (1973). See also L. Esaki, *IEEE Journal of Quantum Electronics* **22**, 1611 (1986).

[2] S. Washburn and R. A. Webb, *Advances in Physics* **35**, 375 (1986).

[3] Y. Aharonov and D. Bohm, *Physical Review* **115**, 485 (1959).

[4] K. Furuya, *Journal of Applied Physics* **62**, 1492 (1987); K. Furuya and K. Kurishima, *IEEE Journal of Quantum Electronics*, **24**, 1652 (1988).

[5] H. Haken and H. C. Wolf, Atomic and Quantum Physics, (Springer-Verlag, New York, 1984); M. G. Legally, Metals Handbook, 9th edn., vol. 10, p. 536 edited by R. E. Whan (American Society for Metals, Metals Park, Ohio, 1986).

[6] A. M. Kriman, G. H. Bernstein, B. S. Haukness and D. K. Ferry, presented at the 4th International Conference on Superlattice, Microstructures and Microdevices held in Trieste, 1988; S. Bandyopadhyay, G. H. Bernstein and W. Porod, to be published in the proceedings of the Conference on Nanostructure Physics and Fabrication, held in College Station, Texas, March 1989.

[7] C. W. J. Beenakker, H. van Houten and B. J. van Wees, to appear in *Europhysics Letters*.

[8] M. E. Heiblum, M. I. Nathan, D. C. Thomas and C. M. Knoedler, *Physical Review Letters* **55**, 2200 (1985).

[9] M. Born and E. Wolf, Principles of Optics, 6th edn., (Pergamon, Oxford, 1980).

[10] M. V. Klein and T. E. Furtak, Optics, 2nd edn., (Wiley, New York, 1986).

[11] Normalization follows by an argument similar to that given in: A. M. Kriman, N. C. Kluksdahl and D. K. Ferry, *Physical Review* B36, 5953 (1987).
[12] A. M. Kriman and P. P. Ruden, *Physical Review* B32, 8013 (1987).
[13] N. Marcuvitz, Waveguide Handbook, vol. 10 of *Radiation Laboratory Series* (McGraw-Hill, New York, 1951).
[14] P. M. Morse and H. Feshbach, Methods of Theoretical Physics, (McGraw-Hill, New York, 1953).
[15] F. W. J. Olver, in Handbook of Mathematical Functions, p. 355, edited by M. Abramowitz and I. A. Stegun (NBS, Washington, D.C., 1964).
[16] D. K. Ferry, G. Bernstein and W.-P. Liu, to appear in Physics and Technology of Submicron Structures, ed. by H. Heinrich, G. Bauer and F. Kuchar (Springer-Verlag, Heidelberg).